

Computer measurement of retinal nerve fiber layer striations

Eli Peli, Thomas R. Hedges III, and Bernard Schwartz

An image analysis method to measure retinal nerve fiber layer (RNFL) striations from digitized fundus photographs was developed to improve detection and monitoring of progressive diffuse RNFL loss. Striations were measured by comparing the high spatial frequency variability across with the variability along the RNFL. This locally normalized measure of striations compensates for the wide density variations both within individuals and between individuals and RNFL photographs. Five repeated measurements were taken at each of three locations from each retinal image. Measurements from five patients with recorded visual field loss due to optic nerve diseases were compared with five normal subjects and five suspect eyes. Measurements clearly distinguished the three groups when taken at the temporal arcades. Measurements above and below the arcades were also consistent, but did not distinguish normals from suspects. The measure was correlated with graded estimates of RNFL integrity of two trained observers ($\rho = -0.57$, $p < 0.001$ and $\rho = -0.61$, $p < 0.001$).

I. Introduction

The diagnostic value of observing nerve fiber damage has been demonstrated for several diseases.¹⁻³ Atrophy of the retinal nerve fiber layer (RNFL) may be focal (i.e., wedge or slit defects) or diffuse. Diffuse atrophy, in which the striated pattern associated with healthy RNFL gradually diminishes, is seen frequently in glaucoma.⁴

Funduscopy and photographic evaluation of RNFL atrophy remains a difficult task, especially for diffuse atrophy, which is the focus of this paper. To improve the evaluation of RNFL photographs, various photographic techniques have been suggested^{5,6} and compared.^{7,8} Recently, methods of enhancing RNFL subjective evaluation using computerized image processing⁹⁻¹¹ have been reported.

Quantitative measurements of RNFL changes were attempted by other investigators. Tagami¹² found a high correlation between the level of visual field loss and graded atrophy of the maculopapillary bundles of the RNFL. The atrophy was estimated subjectively using densitometry of red-free fundus photographs. He classified the atrophy observed with the densitom-

etry into four levels from normal RNFL to total atrophy. In a pilot study, Lundström and Eklundh¹³ measured RNFL atrophy for one patient using computerized densitometry.¹⁴ They used a variability measure defined as the mean of absolute differences between adjacent density values along arcs concentric with the optic disk as a measure of RNFL atrophy. This measure is highly sensitive to contrast and luminance changes between images.

We have expanded and modified this approach using similar measurements and image processing. We used a measure of variability that is locally normalized to compensate for the wide range of densities between fundus photographs taken at different times. These variations arise from changes in illumination related to pupillary size and the local density variability within each photograph due to background choroidal vasculature and pigmentary changes. The compensation is achieved by comparing the density variability measured across the RNFL with that along the RNFL within the same fundus area.

II. Materials and Methods

A. Photo Selection and Digitization

Black-and-white photographs of the RNFL were obtained from patients with optic nerve diseases and normal volunteers using a Canon CF-60Z fundus camera and Plus X film (Kodak ASA 100) with a green Spectrotech-540 filter. Photographs were taken separately of the inferior and the superior temporal arcades with the optic nerve head at the corner of each frame.

The authors are with Tufts-New England Medical Center, Department of Ophthalmology, Boston, Massachusetts 02111.

Received 1 June 1988.

0003-6935/89/061128-07\$02.00/0.

© 1989 Optical Society of America.

Field size was adjusted to $\sim 30^\circ$. Negatives were digitized with a linear array camera (Datacopy, Mountain View, CA). Only retinal areas with corresponding visual field defects, as observed from the patients' records, were used. Either inferior or superior quadrants were used from the normal volunteers. All the negatives were positioned for digitization so that the optic disk was at the lower left corner (to appear as a left superior temporal arcade). The image, digitized at a resolution of 512×512 pixels, included about a $15^\circ \times 15^\circ$ section of the negative excluding the round edges. Illumination was adjusted to obtain the maximal contrast for the presentation of the RNFL in the digitized image, resulting in many cases in saturation of the optic disk details. Images were stored on magnetic disks on a VAX 780 computer (Digital Corporation, Maynard, MA) and displayed on a DeAnza (Beverly Hills, CA) IP-5000 image display system. Results were photographed using a Dunn MultiColor camera (Dunn Instruments, San Francisco).

B. Orientation of Measurements

Lundström and Eklundh¹³ performed the densitometry along arcs centered at the optic disk, while Tagami's¹² densitometric readings were taken along a straight line across the maculopapillar bundle. We have noted that, although the retinal nerve fiber striations radiate from the optic disk, the fibers' apparent convergence at 2–3 disk diameters from the margin of the optic disk appears to be much smaller than a direct projection to the center of the nerve head. When we attempted to measure the apparent center of RNFL intersection by measuring two points along two different clear nerve fiber striations and calculated the point where these two lines would intersect, we found that, within the accuracy of this measurement technique and sampling resolution, the fibers appeared to be nearly parallel 2–3 disk diameters from the optic disk. Therefore, measurements were performed for the rest of this study along straight lines rather than arcs and radii.

C. Average Densitometry

Density values representing the fundus reflectivity were taken along straight lines that were drawn across (perpendicular to) the RNFL striations. Brightness values taken along each line generated a vector \mathbf{x}_i :

$$\mathbf{x}_i = (x_{i,1}, x_{i,2}, \dots, x_{i,n}). \quad (1)$$

A number of vectors were taken this way from a set of parallel contiguous lines, separated by 1 pixel in the orthogonal direction, generating a matrix \bar{X} :

$$\bar{X} = \begin{pmatrix} x_{1,1} & x_{1,2} & \dots & x_{1,n} \\ \cdot & \cdot & \dots & \cdot \\ \cdot & \cdot & \dots & \cdot \\ x_{i,1} & \cdot & \dots & \cdot \\ \cdot & \cdot & \dots & \cdot \\ \cdot & \cdot & \dots & \cdot \\ x_{m,1} & \cdot & \dots & x_{m,n} \end{pmatrix} \quad (2)$$

In this matrix, the element x_{ij} represents the j th point

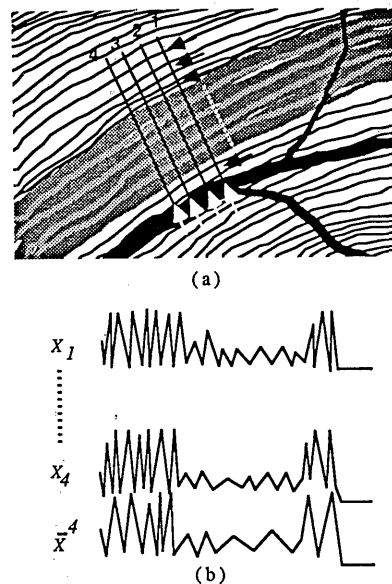


Fig. 1. Schematic presentation of the density averaging technique. (a) Schematic presentation of a retinal nerve fiber layer (RNFL) image with a wedge defect. The grey level information is sampled along lines perpendicular to the RNFL pattern (open arrows). The grey levels are averaged along lines parallel to the RNFL (dark arrows). (b) The average data from four curves generate one curve representing the grey levels across the RNFL (black in the image is represented by low level on the curve and white by high). This final, lowest curve is the averaged density curve used to evaluate the RNFL striations.

on the i th line. This method of representing data is similar to that of Lundström and Eklundh.¹³

To reduce noise effects in the image, we applied an averaging procedure. Noise in the RNFL images may be photographic from film grain or of electronic origin arising from the digitization process, among other less obvious sources. The averaging procedure was applied assuming that the noise is randomly distributed in all orientations, i.e., isotropic, while the RNFL striations are arranged orderly in almost parallel lines. The averaging was thus calculated from values taken along the RNFL over m consecutive lines resulting in a new vector representing an average of order m :

$$\bar{X}^m = (\bar{x}_1^m, \bar{x}_2^m, \dots, \bar{x}_n^m), \quad (3a)$$

where

$$\bar{x}_j^m = \frac{1}{m} \sum_{i=1}^m x_{i,j}. \quad (3b)$$

This average densitometry improves the signal-to-noise ratio in the same way that visually evoked response signals improve with averaging. The averaging technique is illustrated in Fig. 1.

Averaging was expected to reduce noise only for a limited number of lines, because curvature of the RNFL striation reduces alignment between the RNFL and the averaging direction. To find the optimal number of lines that should be averaged to improve signal-to-noise ratio without undesirable deterioration of the signal, we calculated the difference between

consecutive cumulative averages over 20 lines on a number of images. The difference between consecutive cumulative averages was defined as

$$\text{diff}(m) = \sum_{j=1}^n (\bar{x}_j^{m+1} - \bar{x}_j^m). \quad (4)$$

If the averaging operation is ideal, the difference, $\text{diff}(m)$ should decrease asymptotically toward zero as m increases. However, in our experiments we found that $\text{diff}(m)$ decreases up to $m = 4$ or 5 and then converges to an asymptotic value, suggesting that the benefit of line averaging is limited to averaging of four to five lines (Fig. 2).

D. Variability Measure

The variability measure was defined in the following way: The operator using a cursor driven by a graphic bit-pad identified a rectangular area in the digitized photograph that had one side oriented along the RNFL. A series of lines across the RNFL separated by 5 pixels and a similar series of lines along the RNFL were then delineated automatically by the computer (Fig. 3). Note that a separate matrix X is associated with each of these lines. An average densitometry measurement for each line was calculated using two contiguous lines on each side for a total of a five-line width as described in Eq. (3). This assigns a densitometry value to a line position centered in the area from which it was calculated, e.g., if the averaging in Fig. 1 would be carried on only three lines, the averaged values assigned for the position of line 2 will be composed from the values of line 2 together with lines 1 and 3. Similarly, the values assigned for line 3 will be calculated from densitometry measurements of lines 2, 3, and 4.

A variability measure (var) was calculated for each averaged densitometry line in both directions across and along the RNFL. The variability was calculated as:

$$\text{var} = \sqrt{\frac{1}{n-1} \sum_{j=1}^n (\bar{x}_j^m - \bar{x})^2}, \quad (5a)$$

where

$$\bar{x} = \frac{1}{n} \sum_{j=1}^n \bar{x}_j^m \quad (5b)$$

is the mean density for each line.

The resulting two series of variability measurements, one taken from all lines across the RNFL and one taken along the RNFL, were used to evaluate its state. It was assumed that if clear RNFL striations exist in that section of the fundus image, the variability of densities measured across the RNFL should be significantly larger than those measured along it. A paired t-test was then carried out on these two series of measurements to determine the confidence level of the difference. The q value¹⁵ indicating the significance of the difference between the variabilities taken in the two orthogonal directions is used as the measure of RNFL striation in this study.

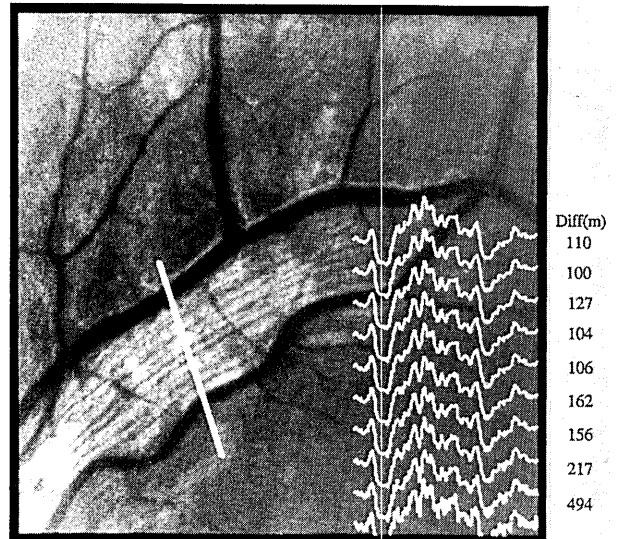


Fig. 2. Illustration of the effect of cumulative averaged density. The bright line across the retinal nerve fiber layer striations represents the area from which the densitometry measures were taken. The curves on the right represent the cumulative averaged density. The lowest curve is the measurement from one line only, the second curve the average of two lines, the third the average of three lines, etc. Note that there are only minor changes in the curves after three averages. The numbers on the right represent $\text{diff}(m)$ for the corresponding pair of averaged density curves.

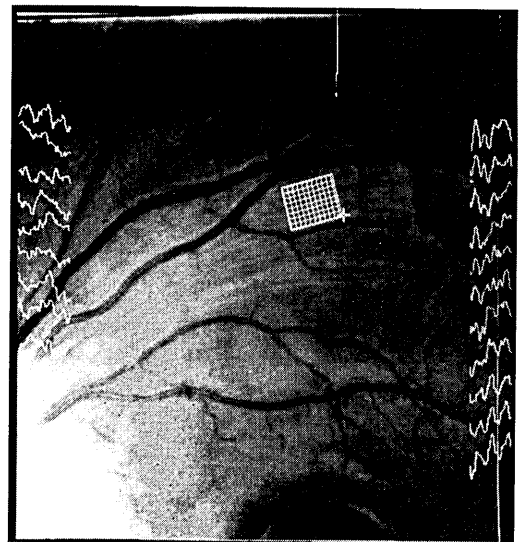


Fig. 3. Variability measurements illustrated for a normal retina. The rectangular area in the arcade represents the area from which measurements were taken. The density curves on the right are from measurements across the retinal nerve fiber layer (RNFL), and the curves on the left from measurements along the RNFL.

A preliminary set of experiments resulted in frequent failure to identify significant RNFL striations, although the densitometry curve displayed on the screen appeared to have a clear high frequency oscillatory pattern in the density taken across the RNFL and not in those taken along it (Fig. 3). The reason for this apparent failure of the variability measure was identi-

fied as large, low frequency variability in the density of all curves, which resulted from underlying variations in choroidal pigmentation, rather than variations in the RNFL pattern. These choroidal variations mask the RNFL variations. The background changes in density, although large in amplitude, are easy to distinguish from the RNFL pattern by observation, because these changes are composed of significantly lower frequencies than the changes associated with RNFL. We correct for these in the following way: each density curve was averaged using a running average window that tracked the changes representing choroidal low frequency noise in the curves but was unable to follow the abrupt changes resulting from the RNFL pattern. The window implemented was a raised cosine [Eq. (6b)] with a length of 17 ($k = 8$), while the average width of a RNFL striation in our images was ~ 3 – 4 pixels for normal eyes. The root mean squared difference of the density from the average smooth density curve was then calculated as the new variability measure of order k , var^k . This effect is illustrated in Fig. 4:

$$\text{var}^k = \sqrt{\frac{1}{n-1} \sum_{j=1}^n (\bar{x}_j^m - \bar{x}_j^k)^2}, \quad (6a)$$

where k represents half of the size of the averaging window and

$$\bar{x}_j^k = \frac{\sum_{l=-k}^{+k} \left(1 + \cos \frac{\pi l}{k}\right) \bar{x}_{j+l}^m}{\sum_{l=-k}^{+k} \left(1 + \cos \frac{\pi l}{k}\right)} \quad (6b)$$

is the raised cosine weighted running average.

E. Subjects

To evaluate the performance of this normalized variability measure, two operators separately processed digitized images from five normals, five patients with RNFL loss that was collaborated with visual field loss, and five suspect eyes. The normal controls were paid volunteers ranging in age from 20 to 45 who underwent complete eye examinations prior to photography, except for intraocular pressure measurements that were deferred to follow the photographic session. The volunteers included two women and three men, one of whom was black. The patients had optic nerve diseases with documented field loss with Octopus 2000 R automated perimetry. The patients were a 14-yr old girl with secondary open-angle glaucoma, a 32-yr old woman with low-tension glaucoma, a 54-yr old man with open-angle glaucoma, a 65-yr old woman with open-angle glaucoma, and a 56-yr old woman with idiopathic optic neuropathy. The diagnosis of glaucoma was determined clinically. Glaucoma patients had visual field loss by Octopus programs 7 and 31, recorded nerve head changes characteristic of glaucoma, and, except for the low-tension case, all had pressures of more than 21 mm Hg on repeated evaluations. Visual field loss was defined as a difference of 10 dB or more from the age-corrected normal values, at a cluster of three or more contiguous points. Although RNFL

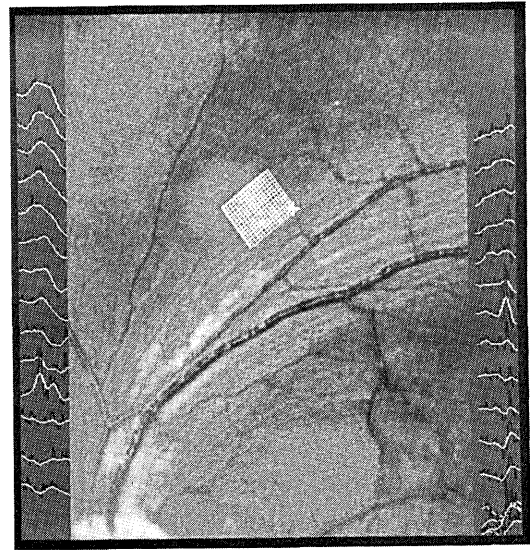


Fig. 4. Illustration of the corrected variability measurements for normal retinal nerve fiber layer (RNFL). The dark curves represent the density measurements taken as in Fig. 3. The white curves represent the running average curve described in Eq. (6b). The variability is calculated from the difference between the white and dark curves. Note that the variability on the right (across the RNFL) is larger than that on the left (along the RNFL).

evaluation is now used routinely in evaluating glaucoma patients at our clinic, all these patients had their diagnoses established before we started to use RNFL photography. Glaucomatous visual field loss generally correlated with observed RNFL defects both in location and severity and we analyzed only quadrants corresponding to visual field loss.

Glaucoma suspects were defined as patients with elevated intraocular pressure >21 mm Hg on two independent measurements with no visual field loss as determined by Octopus programs 7 and 31. These patients may or may not have had optic disk changes.

The suspect eyes were those of patients with normal visual fields and the following reasons to suspect diseases: right eye of a 14-yr old girl with ocular hypertension, with the fellow eye diagnosed with secondary open-angle glaucoma; right eye with ocular hypertension of a 50-yr old man with the fellow eye diagnosed as primary open-angle glaucoma; left eye of a 74-yr old woman with high ocular hypertension in both eyes; right eye of a 32-yr old woman with the fellow eye diagnosed with low-tension glaucoma; and the left ocular hypertensive eye of a 65-yr old woman with glaucoma field loss in the fellow eye.

F. Location of Measurements

The processing included repeated measurement of five windows placed in the same approximate area. In each image, three different areas were tested, one above the vascular arcade, one within the temporal arcade, and one below the arcade. The operators were instructed as to the general area of placement of the window and recorded the results of statistical testing on five consecutive automated placements. The ori-

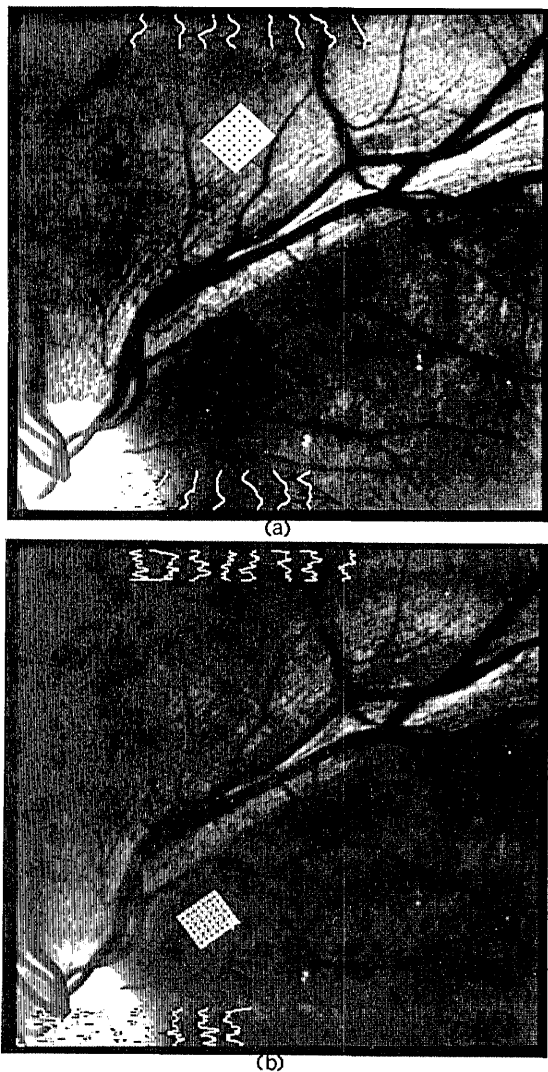


Fig. 5. Comparison of variability measurement in an apparently normal and damaged retinal nerve fiber layer (RNFL) in the same eye of a patient with Leber's optic atrophy. (a) Measurements taken outside the vascular arcade, normal RNFL. The density along the RNFL (bottom) and the density across the RNFL (top). Note that the high spatial frequency variability across the RNFL is larger, even at this measurement area, outside the arcade. The difference is even greater inside the arcade. (b) Measurement in the papillomacular bundle area of advanced diffused atrophy results in variability along which is similar to the variability across the RNFL. Note: the density curves in (a) and (b) are not to the same scale.

entation and size of each area was slightly different. The operators indicated the initial orientation and size of the measurement area by selecting three points. Orientation of the NFL was determined by direct observation and in relation to the vascular pattern. Misalignment by large degrees can affect the results in a substantial manner. However, it is difficult to misjudge the orientation by more than 15° by using the vascular pattern as a cue, even if there are no striations visible. Preliminary experiments that tested the effect of orientation on the variability indicated minimal effects of small angular deviations of $<15^\circ$.

During testing, the program randomly varied the position of the three points within a 5×5 pixel window around the first position. The results of the five measurements were averaged. This procedure was implemented to reduce the sensitivity of the measurement to the exact identification of striation orientation by the operator.

G. Comparison with Trained Human Observers

Two trained observers were presented with the fifteen images in a random masked fashion. The areas of automatic measurements were indicated, and the observers were asked to grade the appearance of the RNFL striations in the marked areas. The optic disk was masked for these presentations. A scale of 0–10 was used, with 10 indicating clear, highly visible, apparently normal RNFL, and 0 indicating total atrophy with no visible striations. The observers were asked to ignore the overall appearance and base their judgments on the specific local appearance of striations.

III. Results

We assumed that healthy RNFL striations will result in a variability of the striated density measure across the nerve fibers that is significantly larger than that measured along the RNFL (Fig. 5). This hypothesis was tested for each set of measurements and the result recorded as the q value.¹⁵ Thus, for healthy RNFL, we expected a very low q value and for severe diffuse atrophy a very high q value ($q > 0.2$). If the variability across the RNFL was smaller than that along it, we defined the q value arbitrarily to be $q = 1.0$. The q values for each of the five measurements taken at each location were averaged to obtain the q value used for comparison.

The average q values from five patients, five normal controls, and five suspect eyes are listed in Table I. The measurements inside the vascular arcade clearly distinguish between diseased and normal eyes. The average q value of $q = 0.0009$ for the normal controls indicates high probability of RNFL striations, while $q = 0.47$ for the diseased eye indicates no difference between the variability measure taken across and along the RNFL in the diseased eyes. The intermediate results for the suspect ($q = 0.15$) indicate a differ-

Table I. Measurements of Retinal Nerve Fiber Layer Striations In Diseased, Suspect, and Normal Eyes

	Diseased	Suspect	Normal
Outside vascular arcade	0.70	0.38	0.33
In vascular arcade	0.47	0.15	0.0009
In papillomacular bundle	0.82	0.16	0.21

Averaged q values for the difference between variability measures taken across and along the retinal nerve fiber layer (RNFL). Low q value indicates clear striation in the direction of the RNFL. High q value indicates lack of difference between the variabilities measured in both directions. Each measurement represents the average of five eyes and five repeat measurements for each eye.

ence between the two directions, but with less apparent striations than the normal eyes.

With the normalization and correction for choroidal density variations, the measurements were consistent with human observation on almost all informal experimental trials. However, occasional misclassifications occurred that usually were the result of including a vessel within the measurement area. If the vessel was along the RNFL, it was identified as a strong striation that would result in assignment of RNFL to areas where they could not be visualized. If the vessel was lying across the RNFL, it resulted in a measurement of strong variation in this direction that negated the effect of the RNFL striations. In many cases, small vessels, which were included in the measurement area, were diagonal to the RNFL, affected both measurements equally, and had little net effect on the final measurement.

Although the measurements outside the vascular arcade and in the papillomacular bundle resulted in higher q values for the diseased eyes than normal eyes, the results were not as conclusive. The average q value for the normal eyes could not be interpreted as indicative of measurable RNFL striations. In most cases, these measurements agree with human observers who could not distinguish striations in the measurement area.

The trained observers had difficulty ignoring the overall appearance of the fundus and evaluating only local striations. They felt that their grading was unavoidably affected by the appearance of other areas. The correlation between the grades given by the observers and the calculated q value at each location was nevertheless significant ($\rho = -0.57, p < 0.001$ and $\rho = -0.61, p < 0.001$) (Fig. 6).

IV. Discussion

Evaluating the RNFL appears to be an important aid to diagnosis and monitoring of optic nerve diseases. Diffuse atrophy is the most common form of nerve fiber loss in glaucoma.⁴ Unfortunately, diffuse RNFL atrophy is difficult to detect, and it is even more difficult to quantify such diffuse changes over time. Preliminary work by Tagami¹² and Lundström and Ek-lundh¹³ has suggested the feasibility of computerized image analysis techniques for measuring RNFL atrophy. We have introduced an improved measurement technique that takes into account a number of confounding variables.

This work assumed that the RNFL pattern may be approximated by linear striations. This assumption allows us to implement a simple noise reduction scheme (directional averaging) and to design a variability measure. On close examination, it became obvious that although the RNFL striations may be less linear than previously depicted in drawings, they closely approximate straight lines over the short distances used in averaging. The small deviations from linearity are part of the inherent noise in the image that necessitates the probabilistic approach used to identify the presence of striations. We use local nor-

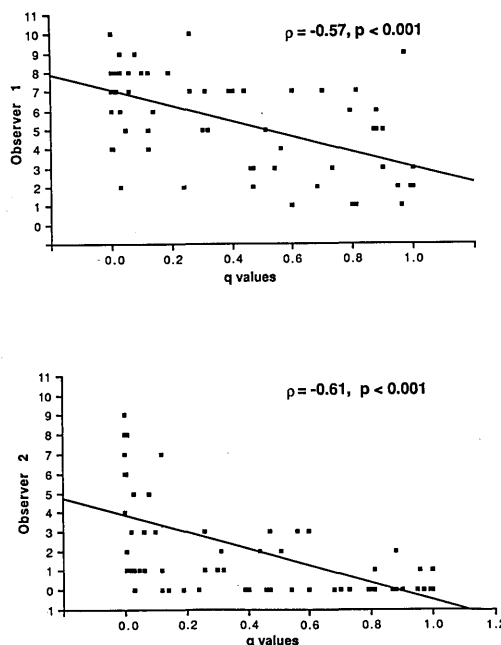


Fig. 6. Correlation between the measured q values and the grading of the retinal nerve fiber layer by two trained observers. Although the observers have different biases, their coefficients of correlation are very similar and both are highly significant despite the apparent variability in the data.

malization to compensate for variation in flash illumination and optical alignment during fundus photography. The line averaging technique compensates for high frequency isotropic noise such as film granularity and electronic noise in the digitizing system. The local normalization that we introduced limits the effect of low frequency local pigmentary changes and the choroidal vascular pattern on measurement of the RNFL. With these controls we can obtain reliable measurements that distinguish between diseased and normal eyes within the vascular arcade. This agrees with previous reports that have indicated visibility of RNFL striations to be much clearer in the vascular arcade than in the papillomacular bundle or the retinal periphery.¹

Our variability measure evaluates only small sections of the retina at a time. The human observer tends to integrate impressions from the whole area of visible retina. Even with this difference, we found highly significant correlations between computerized measurements of RNFL striations and the grading of striations by trained observers' ratings of RNFL integrity. Although within the vascular arcade the technique appears effective enough to be used for diagnosis, our impression is that the main use of this method at this time may be limited to comparing nerve fiber damage over time in the same patient. Our normal subjects were substantially younger than our patient groups. Since ganglion cells are known to decrease in numbers with age (although we know of no direct comparison of the clinical appearance of the RNFL between a younger and older population), our results

should be interpreted with caution until further testing is done. Indeed, a much larger study is necessary to establish the clinical value of our method. Studies evaluating the diagnostic value of imaging techniques are difficult and require large patient and control populations with independent disease criteria.¹⁶ Evaluation of our technique may use visual field defects as such an independent criterion. However, the ultimate value of RNFL evaluation for the diagnosis of glaucoma, either by observer or computer measurement, will be significant only if the diagnosis can precede visual field loss.¹⁷ The lack of other independent criteria will require prolonged prospective evaluation of patients with elevated intraocular pressure to obtain the research material for such a study.

The technique described here as well as common clinical evaluation of the RNFL⁴ is based on 2-D retinal images. The RNFL is known to have measurable depth that decreases with atrophy.¹⁸ Stereoscopic images of the retina were used first by Manor *et al.*¹⁹ to qualitatively evaluate the RNFL integrity. Recently, Takamoto and Schwartz²⁰ showed that stereogrammetry of the RNFL is feasible and may be a sensitive measure of atrophy. However, automated depth measurements are very difficult because of the transparent appearance of the RNFL and represent a great challenge to computer vision techniques.

Quantitative analysis of RNFL images is limited by the quality of the images. Image currently obtained through digitization of films taken with standard fundus cameras are poor in contrast and resolution. With the development of scanning laser ophthalmoscopes (SLO), which are specifically tuned to imaging of the RNFL,^{21,22} the contrast and the resolution are expected to improve dramatically, resulting in increased reliability of all image-processing techniques. We plan to evaluate our technique using images obtained from a fully confocal SLO²² in the near future.

This work was supported in part by grants EY05450 and EY05957 from the National Institutes of Health, Bethesda, MD.

E. Peli also works at the Eye Research Institute and Harvard Medical School.

References

1. W. F. Hoyt, L. Frisén, and N. M. Newman, "Funduscopy of Nerve Fiber Layer Defects in Glaucoma," *Invest. Ophthalmol.* **12**, 814 (1973).
2. A. Vannas, C. Raitta, and S. Lemberg, "Photography of the Nerve Fiber Layer in Retinal Disturbances," *Acta Ophthalmol.* **55**, 79 (1977).
3. M. Lundström and L. Frisén, "Atrophy of Optic Nerve Fibres in Compression of the Chiasm; Degree and Distribution of Ophthalmoscopic Changes," *Acta Ophthalmol.* **54**, 623 (1976).
4. A. Sommer *et al.*, "Evaluation of Nerve Fiber Layer Assessment," *Arch. Ophthalmol.* **102**, 1766 (1984).
5. A. Sommer, S. A. D'Anna, H. A. Kues, and T. George, "High-Resolution Photography of the Retinal Nerve Fiber Layer," *Am. J. Ophthalmol.* **96**, 535 (1983).
6. A. Sommer *et al.*, "Cross-Polarization Photography of the Nerve Fiber Layer," *Arch. Ophthalmol.* **102**, 864 (1984).
7. P. J. Airaksinen, H. Nieminen, and E. Mustonen, "Retinal Nerve Fiber Layer Photography with a Wide Angle Fundus Camera," *Acta Ophthalmol.* **60**, 362 (1982).
8. E. Peli *et al.*, "Nerve Fiber Layer Photography: a Comparative Study," *Acta Ophthalmol.* **65**, 71 (1987).
9. E. Peli, T. R. Hedges, and B. Schwartz, "Computerized Enhancement of Retinal Nerve Fiber Layer," *Acta Ophthalmol.* **64**, 113 (1986).
10. E. Peli, "Adaptive Enhancement Based on a Visual Model," *Opt. Eng.* **26**, 655 (1987).
11. S. Mitra, B. S. Nutter, T. F. Krile, and R. H. Brown, "Automated Method for Fundus Image Registration and Analysis," *Appl. Opt.* **27**, 1107 (1988).
12. Y. Tagami, "Correlations Between Atrophy of Maculo-Papillar Bundles and Visual Functions in Cases of Optic Neuropathies," *Doc. Ophthalmol. Proc. Ser.* **19**, 17 (1979).
13. M. Lundström and J-O. Eklundh, "Computer Densitometry of Retinal Nerve Fibre Atrophy: a Pilot Study," *Acta Ophthalmol.* **58**, 639 (1980).
14. The term densitometry is used here for measurements of reflectance gray levels rather than the common use for $\log(1/T)$, where T is the transmission fraction.
15. The q value used here is equivalent to the p value commonly used to denote the confidence level in a difference between two measured variables.
16. J. A. Swets and R. M. Pickett, *Evaluation of Diagnostic Systems Methods from Signal Detection Theory* (Academic, New York, 1982).
17. H. A. Quigley, "Examination of the Retinal Nerve Fiber Layer in the Recognition of Early Glaucoma Damage," *Trans. Am. Ophthalmol. Soc.* **84**, 920 (1986).
18. H. A. Quigley and E. M. Addicks, "Quantitative Studies of Retinal Nerve Fiber Layer Defects," *Arch. Ophthalmol.* **100**, 807 (1982).
19. R. S. Manor *et al.*, "Narrow-Band (540-nm) Green-Light Stereoscopic Photography of the Surface Details of the Peripapillary Retina," *Am. J. Ophthalmol.* **91**, 774 (1981).
20. T. Takamoto and B. Schwartz, "Photogrammetric Nerve Fiber Layer (NFL) Thickness Measurements in Normal, Ocular Hypertensive (OH), and Glaucomatous (OAG) Eyes," *Invest. Ophthalmol. Vis. Sci.* **29**(suppl), 421 (1988).
21. A. Plesch, U. Klingbeil, and J. Bille, "Digital Laser Scanning Fundus Camera," *Appl. Opt.* **26**, 1480 (1987).
22. R. H. Webb, G. W. Hughes, and F. C. Delori, "Confocal Scanning Laser Ophthalmoscope," *Appl. Opt.* **26**, 1492 (1987).